QUARTERLY JOURNAL OF THE ROYAL METEOROLOGICAL SOCIETY
Q. J. R. Meteorol. Soc. **00**: 1–9 (0000)
Published online in Wiley InterScience
(www.interscience.wiley.com) DOI: 10.1002/qj.000

Flow Dependency of Background Errors and their Vertical Correlations for Radiance–Data Assimilation

Reinhold Hess
Deutscher Wetterdienst, Postbox 100465, 63004 Offenbach, Germany

Abstract: The present paper examines the dependency of background error statistics on synoptic conditions and flow patterns. Error variances and vertical correlations of background temperatures as used for variational radiance–data assimilation are estimated for two different weather regimes over Europe using the NMC–method and real observations, i. e. radiosonde data and microwave satellite radiances. Results are generalised with half a year of global data from the ECMWF forecasting system, where weather conditions are distinguished using model fields of windspeed, mean sea level pressure, and vorticity. Strong winds and cyclonal flow generally induce larger background errors of 500 hPa temperature and broader temperature correlations with other tropospheric levels than calm wind, high pressure, and anticyclonal flow. Copyright © 0000 Royal Meteorological Society

KEY WORDS variational assimilation, satellite radiances, NMC–method

Received September 4, 2009

1 Introduction

Model background errors in terms of variances and covariances play an essential role in variational data assimilation. The often claimed optimality of variational solutions is guaranteed only if several conditions are fulfilled, that include, among others, the correctness of background error specification. The specification of these errors is difficult, however. Collocations of background fields with radiosonde data were used (e. g. Watts and McNally, 1988), but radiosonde error and error of representativeness contribute to the statistics and in general the number of collocations is poor over sea and in the southern hemisphere, which limits statistical significance. Often background error statistics are derived from differences of short range forecasts with different forecast range, however same valid time (NMC–method, Parrish and Derber, 1981), therefore. The technical implementation is straight forward and the results are useful, the theoretical justification, however, is difficult (Bouttier, 1994). Nevertheless, the statistical NMC–method provides reasonable estimates of background error variances and covariances that have been applied in many variational assimilation schemes. Alternatively also differences from ensemble forecasts are used (e. g. Buehner, 2005) and resulting background error statistics are applied at the European Centre for Medium–Range Weather Forecasts (ECMWF, Fisher and Andersson, 2001).

With the NMC–technique the grid point results are usually averaged over latitude and time and in doing so also over all synoptic conditions and flow patterns. Results of the method for the forecasting system of the ECMWF show a clear dependency of background errors on latitude (McNally, 2000 and Fig. 8). Two regimes of error correlations can be distinguished, the tropics and the extra tropics, that are separated at about 40^o latitude north and south with a seasonal shift of about 10^o to 15^o. For the individual case and grid point the background errors can differ essentially, however, which results in potentially suboptimal use of satellite radiances. Therefore, the interest in adapted and flow dependent background error estimates has increased in recent years. The estimation of background errors at individual grid points by a Kalman filter (Kalman, 1960, e. g. Cohn, 1997) is in general too costly for operational weather forecasting. Developments of more efficient derivates such as ensemble Kalman filtering (e. g. Evensen, 1994 or Evensen, 2003) or local ensemble transformed Kalman filter (Ott *et al.*, 2004) exist.

Not only the specification, also the application of adaptive background errors within variational assimilation schemes is technically and mathematically demanding. Once the adapted background errors are derived, its usage poses severe constraints on the design of the variational assimilation system as the resulting background error covariance matrix must be positive definite and because it has to be inverted efficiently (together with added observation errors or not) in any formulation. Physical space assimilation schemes (PSAS, minimisation takes place in observation space, see Daley and Barker, 2001) are better suited to use adaptive background errors (Courtier, 1997). This is important for 3D-Var systems; within 4D–Var the background errors are implicitly evolving in model time, but their initial values are usually reset every time for the next 4D–Var cycle and a better initialisation should be beneficial as well.

Vertical background error correlations are especially important for the assimilation of satellite soundings, because of their limited vertical resolution on their own. These correlations describe the vertical distribution of information and are crucial in order to retrieve optimal vertical resolution from the new generation hyperspectral infrared instruments (AIRS, IASI), which is still low

compared to topical model resolutions with 90 and more vertical levels and also compared to radiosonde data.

Section 2 of the presented paper compares vertical background error structures of a stable high pressure area with fair weather conditions with errors derived for a stormy scenario with strong westerly winds and lots of rain over Europe. Results obtained from the NMC–method are confirmed using radiosonde data and AMSU–A microwave radiances. In Section 3 global conditional background error estimates based on the NMC–method are compared for different synoptical conditions that are distinguished by various model variables. Section 4 provides conclusion together with an outlook towards parameterisation of background errors using suitable model variables as predictors.

2 Background errors of two different synoptical conditions over Europe

Two test cases are selected that are representative for two very different weather regimes. The first period is 3–9 August 2003 that shows a large and stable high pressure area over central Europe with low winds and high surface temperatures. The second period is 6–12 January 2004 with strong persistent westerly winds and lots of rain. Averages of 500 hPa geopotential heigh and windspeed are displayed for period one and two in Fig. 1 and 2, respectively.

2.1 Background statistics derived from NMC–method

Mean background error variances and mean vertical covariances of temperature of the two periods and given domain are estimated by 48 h-24 h differences of ECMWF forecasts using the NMC–method (no further scaling of differences is applied). In areas with low data coverage and further downstream the NMC-method has potential problems, because in these cases the shorter range forecast does not benefit much from the later analysis it is started from. Over Europe data coverage is high and results of the NMC-method are considered reasonable.

The vertical distributions of mean error covariances and correlations with the 500 hPa level are presented in Fig. 3. The 500 hPa temperature variance of the stormy scenario in January is about $1.4\,\mathrm{K}^2$, which is much larger than that of the high pressure period in August with only about $0.3\,\mathrm{K}^2$. Also the covariances of 500 hPa with other tropospheric height levels are significantly larger for the period in January, e. g. the covariance with 700 hPa is about $0.64\,\mathrm{K}^2$ in January and negligible in August. Temperature covariances with the stratospheric levels (at 200 hPa) are strongly negative and again much stronger (larger in absolute value) in January.

These stronger error variances and covariances in January can be well explained with a higher variability of the weather regime and with location or phase errors of weather events according to the stronger winds.

Also the correlations are significantly broader in January, which is to be expected when they are induced by large location errors that may dominate the statistics. The 500 hPa–700 hPa correlation is 0.39 in January and 0.055 in August. The correlation of these two levels is considered especially important, since it defines the vertical distribution of information of satellite radiances in the mid and lower troposphere. Forecast quality was found to be very sensitive to errors in this vertical region (McNally 2002). Similar results are obtained e. g. also for the 500 hPa–850 hPa correlations.

Figure 4 shows the mean geographical forecasts distributions of the 500 hPa–700 hPa temperature correlations for the selected periods in August and January. In the August period the correlations are even negative in large parts where the wind speeds are lowest (see Fig. 1). The strong winds in January come along with strong positive correlations exceeding 0.8 (see Fig. 2). The horizontal distribution is rather small scale in both cases, which can be explained by the small sample sizes of only seven days.

2.2 Validation of background error statistics with observations

The qualitative differences of the vertical background error structures are validated in the following with real observations in order to guarantee that they are not related to artefacts of the NMC–method. Innovation statistics (differences between observation and model background equivalents) of radiosonde data and AMSU–A microwave radiances are used to confirm the results of the NMC–method.

These departures include background errors, observation errors, errors of representativity, and in case of radiances also simulation errors. It is possible to separate observation and background errors after Hollingsworth and Lonnberg (1986), Lonnberg and Hollingsworth (1986), or e. g. Desroziers and Ivanov (2001), however, larger samples and longer periods of selected weather regimes would be required. Since it is expected that mainly background errors change depending on the selected scenario, the size of the innovations provides indications on systematic differences of these.

2.2.1 Radiosonde data

Error statistics of radiosonde temperature departures are computed for both periods and the domain given in Fig. 1. Only radiosondes of good quality are sampled that had been operationally assimilated with 4D–Var at ECMWF. This is also true for all latter radiosonde statistics. The data of every radiosonde is binned into 16 pressure levels ranging from 1000 hPa to 5 hPa by averaging all radiosonde level data matching the same pressure bin. In this way each radiosonde has equal weight independently on the number of individual levels of measurement.

Departures of the binned radiosonde data are then computed against model background and analysis of ECMWF 4D–Var*. The vertical distribution of rms temperature departures and the correlations with the 500 hPa

*Because of this binning and averaging of the radiosonde data the computed rms differences decrease compared to statistics based on the

DOI: 10.1002/qj

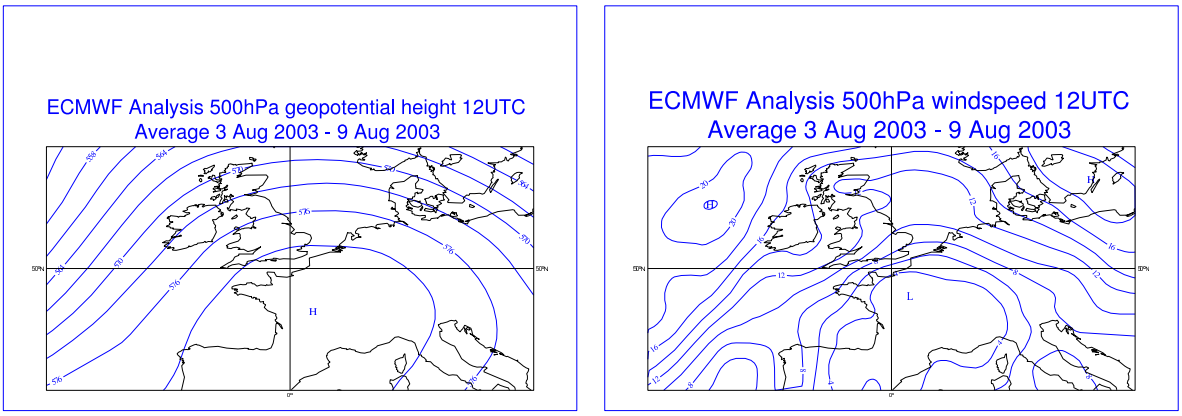

Figure 1. *ECMWF 500 hPa geopotential height (left) and wind speed (right) averages of 0 UTC analysis for period 3–9 August 2003 representing a scenario with low winds and high screen level temperatures. Domain is 40^o to 60^o latitude and -20^o to 20^o longitude covering central Europe.*

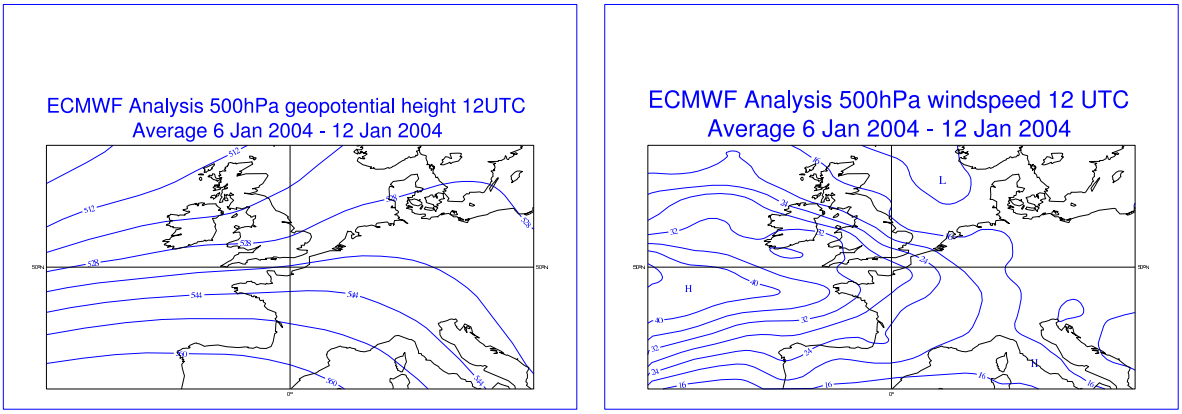

Figure 2. *As Fig. 1, but for period 6–12 January 2004 representing a weather regime with strong westerly winds and lots of rain.*

pressure level for radiosondes valid at 0 UTC are displayed in Fig. 5, for 12 UTC in Fig. 6. For better comparison of the values for selected levels see also Tab. I. The 0 UTC and 12 UTC radiosonde statistics are very similar, the rms errors tend to be slightly larger for 12 UTC and the 500 hPa–700 hPa correlation is weaker at 12 UTC than at 0 UTC in January.

Consistently with the results of the NMC–method, the rms errors of the 500 hPa temperature departures of the winter period are larger than in summer. Again the 500 hPa–700 hPa correlations are larger in winter. Also the negative correlations between 500 hPa and 200 hPa are consistently more pronounced for the winter period.

When comparing radiosonde statistics and the results of the NMC–method (Fig. 3, Tab. I), it seems that rms errors and 500 hPa–700 hPa temperature correlations are very similar in August, whereas in January the NMC–method shows a stronger increase both in rms errors and in the correlations, than the radiosonde statistics. An explanation could be that the NMC–method is based on differences of forecasts that twice include location errors or phase problems, which leads to large and correlated errors that have significant impact on the statistics.

		August		January	
time	level [hPa]	RMS [K]	COR [1]	RMS [K]	COR [1]
radiosondes					
0 UTC	500	0.56	0.01	0.73	0.23
	700	0.55		0.80	
12 UTC	500	0.65	0.00	0.74	0.15
	700	0.60		0.83	
NMC–method					
0 UTC	500	0.55	0.055	1.2	0.39

Table I. *Rms and correlation of radiosonde departures against 4D–Var of ECMWF at 500 hPa and 700 hPa for the summer and winter period as given in Figs. 5 and 6. Because model biases are negligible, the rms values of the NMC-statistic are based on the variances as shown in Fig. 3.*

The analysis departures are displayed as well in Figs. 5 and 6, which show how much the fit of the model to the observations is improved by the analysis compared to the background. In general the rms of the 500 hPa temperature analysis is between 0.4 K and 0.5 K, that is an

full set of available level data. Correlations between any two vertical bins are computed for all radiosondes that covers these two bins, not necessarily all the other bins as well. In this way also radiosondes that do not cover a complete accent can be used and the sample size is essentially increased. The resulting correlations become statistically more significant in this way. The computed correlation matrix remains symmetric, however, not necessarily positive definite.

DOI: 10.1002/qj

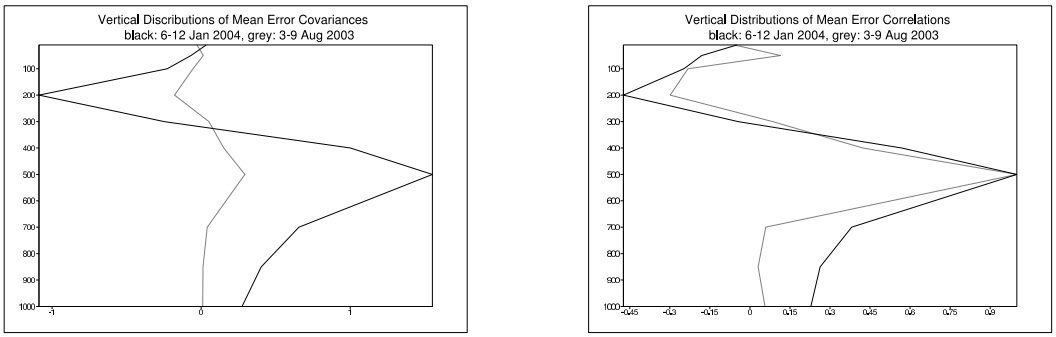

Figure 3. *Distributions of vertical temperature error covariances (left) and correlations (right) with 500 hPa level according to NMC–method for the scenarios in January (black) and August (grey). Domain as in Figs. 1 and 2.*

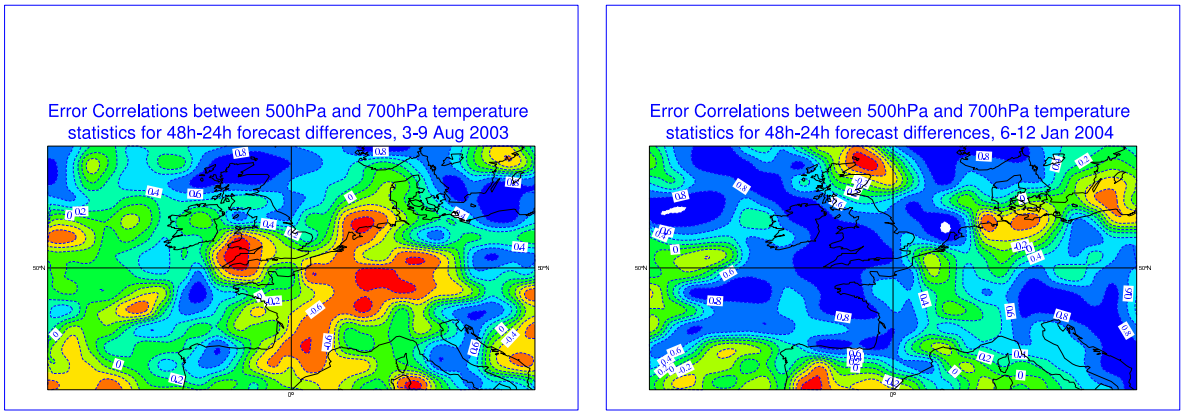

Figure 4. *Geographical distribution of temperature error correlations between 500 hPa and 700 hPa as estimated with 48 h-24 h forecast differences of ECMWF using the NMC–method in August (left) and January (right).*

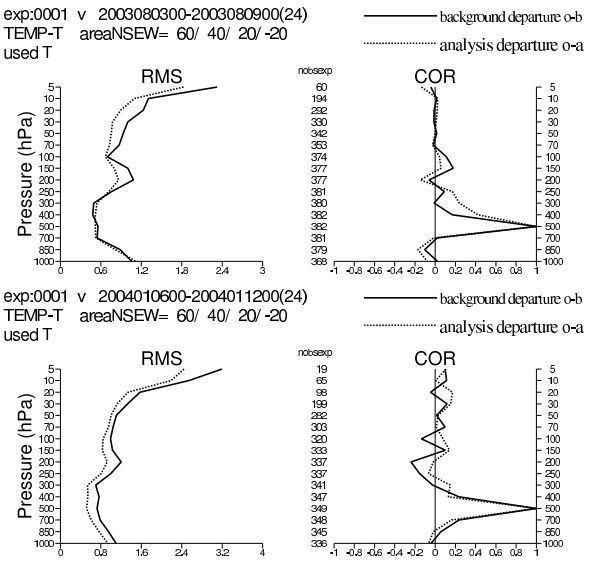

Figure 5. *Rms temperature departures of radiosonde data against ECMWF 4D–Var background and analysis and correlations of departures with 500 hPa level. Background departures are in solid lines, analysis departures are dashed. Radiosondes are valid at 0 UTC. Summer (top) and winter (bottom) period. The reported radiosonde observations at individual levels are binned into the given pressure levels. The number of observations represent the number of radiosondes, therefore, rather than the total number of reports at individual levels.*

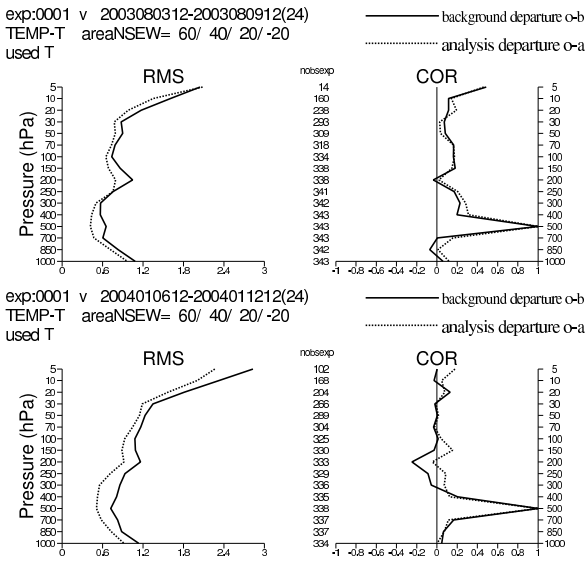

Figure 6. *Same as Fig. 5 but for radiosondes valid for 12 UTC.*

upper limit for the error of representativity. The observation error of radiosondes that includes representativity is 0.76 K at ECMWF for the system being used. The smaller background departures in August thus have a significant contribution from observation errors, the increase in January is caused by larger background errors.

As a conclusion of this section it can be stated

DOI: 10.1002/qj

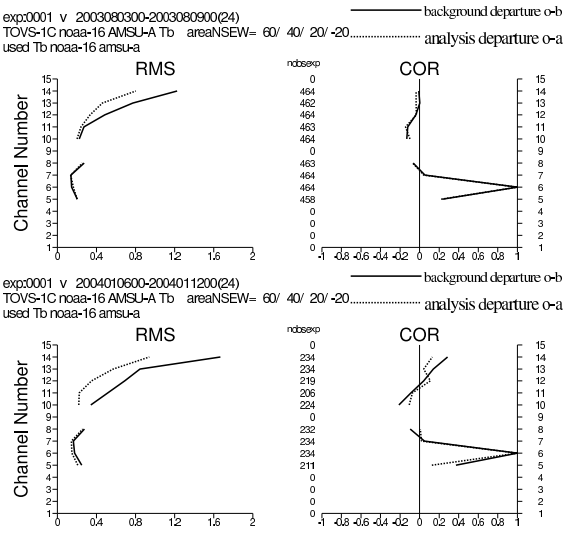

Figure 7. *Rms brightness temperature departures and correlations with Channel 6 of AMSU–A of NOAA–16. Summer (top) and winter (bottom) period. Background departures are in solid lines, analysis departures from ECMWF 4D–Var are dashed. Radiances are valid around 0 UTC.*

that the radiosonde statistics confirm the results of the NMC–method, which indicates that model errors in the troposphere are larger and broader for the period in January than in August, although the signal is smaller for the radiosonde statistics.

2.2.2 AMSU–A radiances

In the following also satellite radiances are used to validate the theory of different forecast error structures for different synoptical situations. Brightness temperature departures of AMSU–A of NOAA–16 are computed for the selected time periods and domain, and rms differences are presented together with correlations of Channel AMSU–A 6 in Fig. 7. Channel 6 has its highest sensitivity at about 400 hPa, Channel 5 peaks at about 750 hPa with considerable impact from surface emissivity. The rms differences are small in general (Tab. II) compared to the radiosonde departures (Tab. I). Because of the broad weighting functions and their implicit averaging, the microwave departures are not quantitatively comparable to the in situ measurements of the radiosondes. Moreover, the sensitivity of Channel 5 (and to a small extent also of Channel 6) to surface emission may affect the statistics. The size of the temperature departures, nevertheless, correspond well to the assumed observation errors for Channels 5 and 6 of 0.25 K of ECMWF.

The results confirm that the departures are larger for the period in winter. Also the correlations between Channel 5 and 6 are not strictly comparable to those of the radiosonde departures, however, the signal of the broader correlations in the troposphere in winter is qualitatively confirmed. Significance of these results, that are based on periods of one week only, will be addressed in Sec. 3.

	August		January	
Channel	RMS [K]	COR [1]	RMS [K]	COR [1]
5	0.21	0.22	0.25	0.37
6	0.15		0.19	

Table II. *Rms and correlation of departures of Channels AMSU–A 5 and 6 of NOAA–16 for the summer and winter period in the northern hemisphere as shown in Fig. 7.*

3 Global conditional error statistics

The findings of Sec. 2 on the dependency of background errors on synoptic conditions are restricted so far to two selected time periods and the domain covering Europe. In this section the previous results are generalised with global statistics based on ECMWF model fields with a resolution of $5^o \times 5^o$ for 0 UTC aplying the NMC–method again. Half a year of data, i. e. April to September 2003, is used to provide statistically significant sample size.

Figure 8 shows 500 hPa temperature standard deviation and its correlation with the 700 hPa level for all weather conditions. The results correspond to those given in McNally (2000): There are two regimes with very different error structure, the tropics and the extra tropics. In the tropics the standard errors are smaller and the correlations are sharper. The latter is shown here for 500 hPa–700 hPa correlations, but it is similar for correlations between other tropospheric levels as well. The dependency on latitude is commonly known and already accounted for in variational data assimilation schemes. In this and all later NMC–statistics biases are negligible compared to the shown standard deviations.

In the following sampling of NMC–statistics is carried out in depedence of analysed model fields of wind speed, mean sea level pressure, and vorticity in order to select different weather conditions and to generate conditional background error statistics. Other variables including cloud coverage at different height levels habe been tested as well, but the results are less significant and they are not presented in detail, therefore.

3.1 Windspeed

The data of half a year has been sampled for situations with windspeed at 500 hPa exceeding $15\,\mathrm{m\,s^{-1}}$ and being lower than $10\,\mathrm{m\,s^{-1}}$. The resulting standard deviation of 500 hPa temperature error and the 500 hPa–700 hPa correlations are displayed in Fig. 9. There are only few cases with high wind speeds in the tropics and the results are not shown in these areas, therefore. Likewise there are only few cases with low wind speed in the sea south of Afrika, which is blacklisted as well. In the northern latitudes the standard deviation of 500 hPa temperature forecast error is significantly larger for high wind speed with values around 1.4 K in comparison with low wind speed and errors about 0.8 K in average. Similarly in the southern latitudes, however, the signal is weaker. Also the 500 hPa–700 hPa temperature correlations are stronger for high wind speeds.

DOI: 10.1002/qj

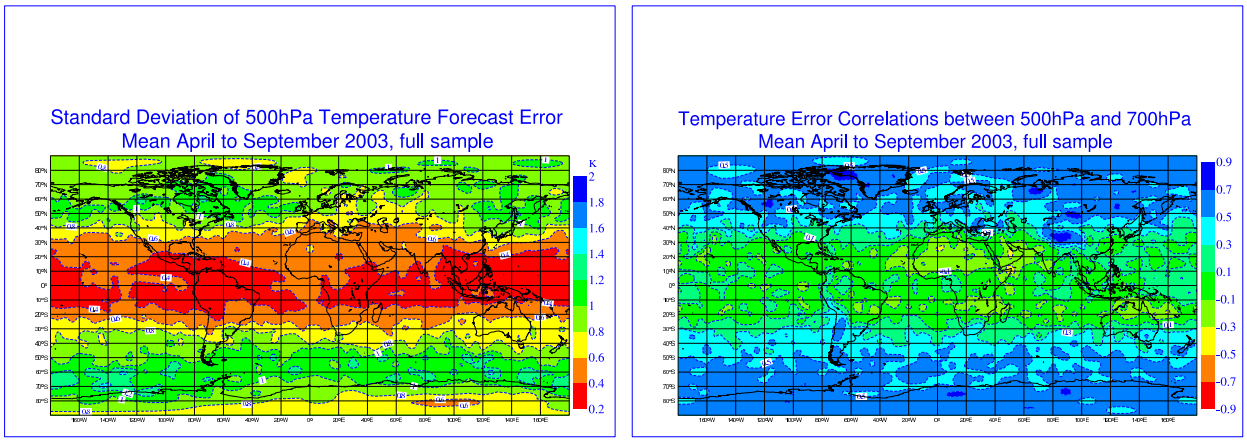

Figure 8. *500 hPa temperature error standard deviation (left) and 500 hPa–700 hPa correlations (right) of 48 h-24 h forecasts of ECMWF valid for the same time, mean from April to September 2003. Geographical sampling is based on a $5^o \times 5^o$ grid. No restriction for special situations is applied.*

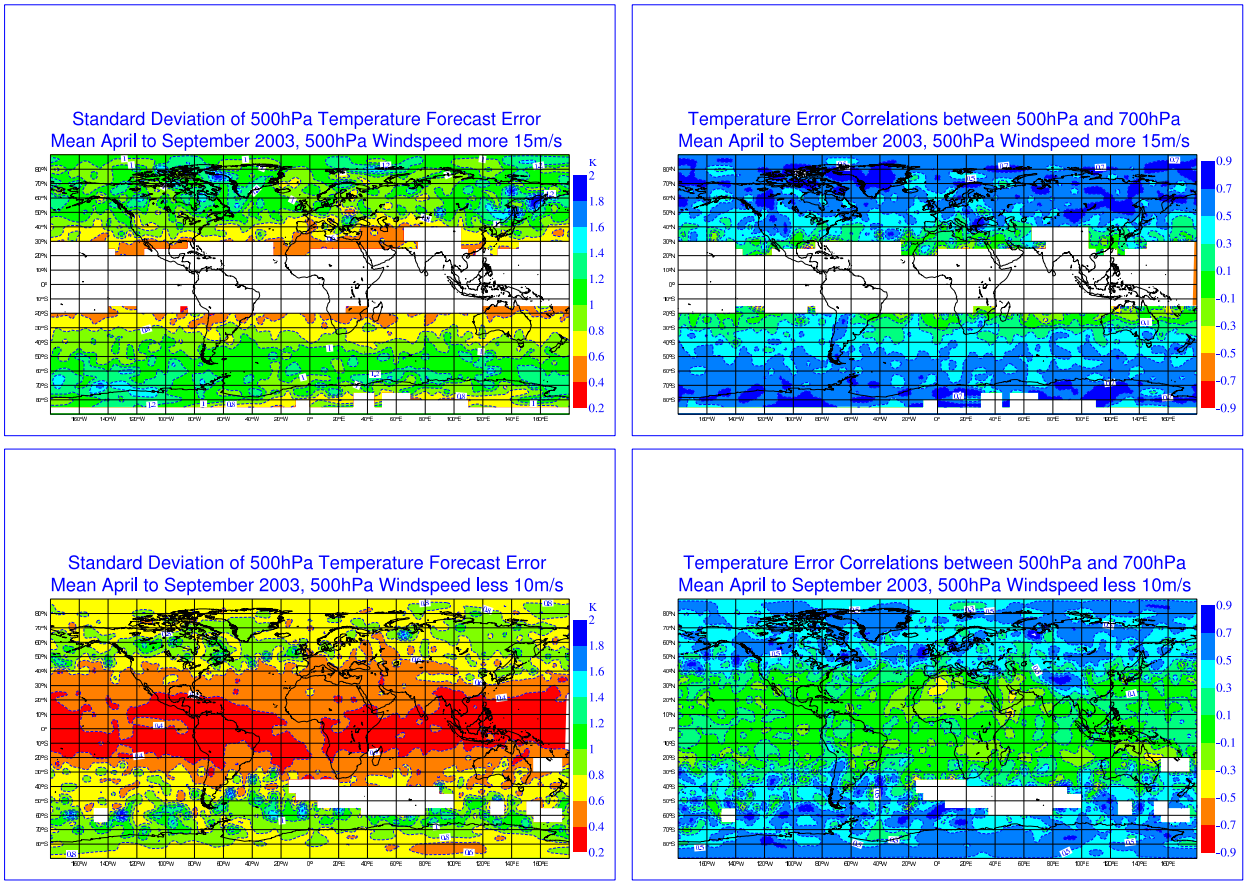

Figure 9. *As Fig. 8, but sampling is restricted to analysed windspeed at 500 hPa more than 15 m s^{-1} (top) and less than 10 m s^{-1} (bottom). Statistics of areas with less than ten samples are considered not significant and kept blank.*

3.2 Mean sea level pressure

Sampling of the statistics depending on mean sea level pressure at the value 1013 hPa shows significantly larger errors for low pressure than for high pressure both in northern and southern high latitudes, see Fig. 10.

The error correlations are slighly larger for low pressure than for high pressure. In most of the tropical areas there are only few cases in either one or the other sample. Nevertheless, the remaining errors and error correlations of the tropics show no significant dependency on mean sea level pressure.

These results for the extra tropics are consistent with those of the separation by wind speed, since low pressure usually comes along with high winds, whereas high pressure areas are more often calm.

3.3 Vorticity

Results of the sampling for vorticity at 500 hPa above 0.4 1/s and below -0.4 1/s are presented in Fig. 11. Strong

DOI: 10.1002/qj

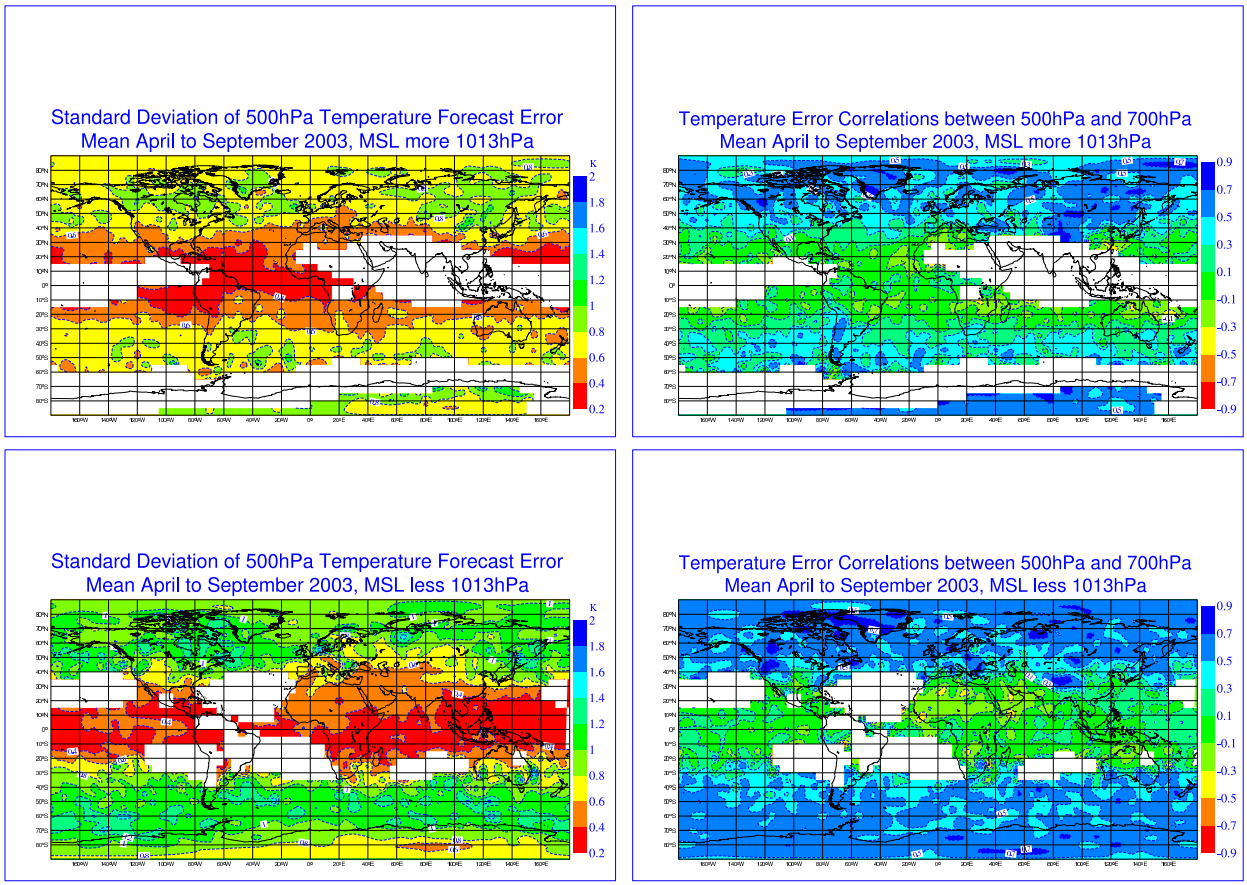

Figure 10. *As Fig. 8, but sampling is restricted to analysed mean sea level pressure more than 1013 hPa (top) and less than 1013 hPa (bottom).*

vorticities (in absolute values) exist only at higher latitudes, no results are obtained for the tropics, therefore. Cyclonal vorticity (positive in the northern and negative in the southern hemisphere) shows mean standard deviation of 500 hPa temperature error of about 1.4 K, whereas it is around 0.7 K, half of size, for anticyclonal flows. This signal of the dependency is stronger than for wind speed and mean sea level pressure, however the selection of cases is more rigorous, since cases with weak vorticity less than 0.4 1/s in absolute value are neglected. The obtained standard deviations correspond well to those of the NMC–method for the selected time periods and European domain, see Tab. I (the biases are negligible). Also the correlations between 500 hPa and 700 hPa show a strong dependency on vorticity. Cyclonal flows, which goes along with low pressure and high wind speeds, induce significantly larger error correlations than anticyclonal scenarios.

This dependency exists also for other levels as well; in Fig. 12 the temperature error correlations between 500 hPa and 300 hPa are presented for the same selection based on vorticity. Cyclonal vorticity results in very strong negative correlations, extremely for the northern, but also for the southern latitudes. The results for the anticyclonal cases are diverse, including strong negative and positive error correlations. In average they are negative, but obviously much weaker than for cyclonal flows.

4 Conclusion and Outlook

It is shown that vertical structure of background errors of ECMWF forecasts significantly depend on the actual weather regime. There are not only systematic differences between the tropics and the extra tropics as commonly accepted, also the synoptic conditions have comparable impact that has been presented for temperature errors at 500 hPa and their error correlations with 700 hPa and other levels. This dependency is shown by studies for selected scenarios over Europe using the NMC–method and with real observations, strictly speaking with radiosondes and AMSU–A microwave radiances. The results are further confirmed and generalised with half a year of global model data from ECMWF by the NMC–method.

In general larger and broader temperature forecast errors exist in the troposphere for synoptic conditions that are in common sense identified as *bad weather*, in terms of model fields defined as high windspeed, low pressure and cyclonal flow, etc. Calm winds, high pressure and anticyclonal flow, commonly related to *fine weather* on the other hand, show much smaller errors and weaker vertical correlations. The larger and broader errors for high windspeeds can be well explained with location errors of synoptical events as already stated in McNally (2000). These location errors may also be the reason that the NMC–method gives significant larger background errors for high winds than the radiosonde departures,

DOI: 10.1002/qj

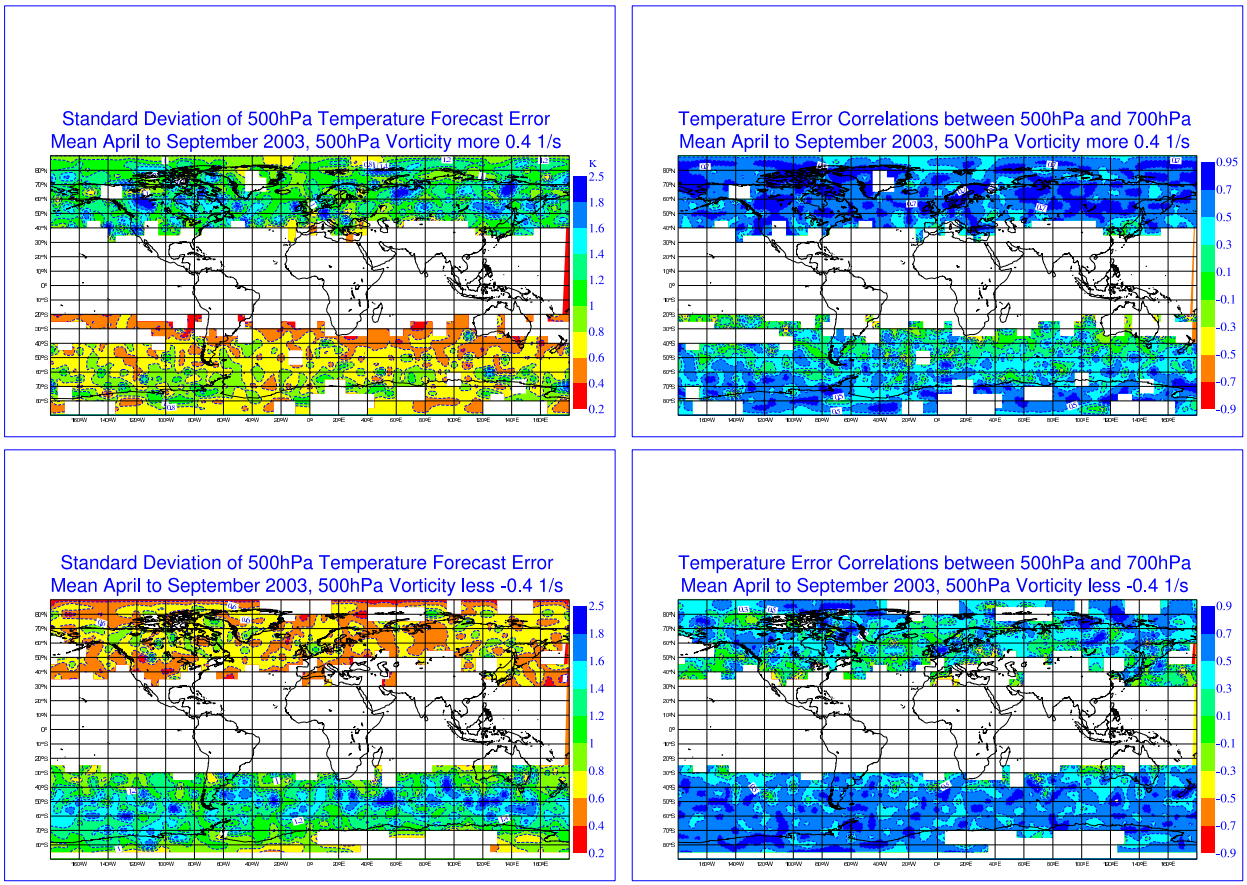

Figure 11. *As Fig. 8, but sampling is restricted to analysed 500 hPa vorticity more than 0.4 1/s (top) and less than -0.4 1/s (bottom).*

since differences of forecasts are evaluated for the NMC–method that both may have location errors. For calm wind the error statistics of radiosonde departures and the NMC–method are similar, but the radiosonde departures could have a significant contribution of the errors of representativity.

In the paper emphasis is given more on qualitative than quantitative dependencies of error statistics especially for the selection of model fields that are used as predictors to select different weather regimes for the global NMC–statistics. The next step would be to find quantitative results and to parameterise background error variances and their covariances depending on the synoptic conditions, where model variables may be used as predictors. The commonly accepted and well established latitude dependency of background errors can likely be related to the weather conditions and treated implicitly in this way. A straight forward approach would be the use of a linear combination of background errors for special conditions based on predictors, where model fields or observations can be used. In the case of e. g. model vorticity φ as predictor, there could be background error correlation matrices for the tropics $\mathcal{C}_{trop}$ and for cyclonal and anticyclonal vorticity in the extra tropics $\mathcal{C}_{cyc}$ and $\mathcal{C}_{acyc}$, respectively. The parameterised background error correlation matrix could be a homotopy like

$$\mathcal{C}(\varphi) = (1-|\varphi|)\,\mathcal{C}_{trop} + \begin{cases} |\varphi|\,\mathcal{C}_{cyc} & \text{for} \quad \varphi \text{ cyclonal} \\ |\varphi|\,\mathcal{C}_{acyc} & \text{for} \quad \varphi \text{ anticycl.} \end{cases}$$

when φ is scaled between -1 and 1.

Once the adaptive background errors are modeled, their application within operational assimilation schemes is also demanding and poses severe technical constraints, especially if not only vertical but also horizontal correlations are considered as well as for 3D– or 4D–Var schemes. It is a major challenge to guarantee that the generated background error covariance matrix remains positive (semi–)definite. It is not required to build and store the matrix as a whole, however, it needs to be inverted efficiently with or without additional terms for the observation errors, depending on the formulation of the applied assimilation scheme. Physical space analysis systems (PSAS) are considered more appropriate to use locally defined background errors and covariances, since background error models can be implemented in a simpler way.

Acknowledgements

Basic parts of the presented work were carried out during two research visits at ECMWF that was financed by EUMETSAT unter the NWP–SAF Visiting Scientist program. Many thanks to the friendly and fruitful guidance by Tony McNally and other colleagues at ECMWF.

DOI: 10.1002/qj

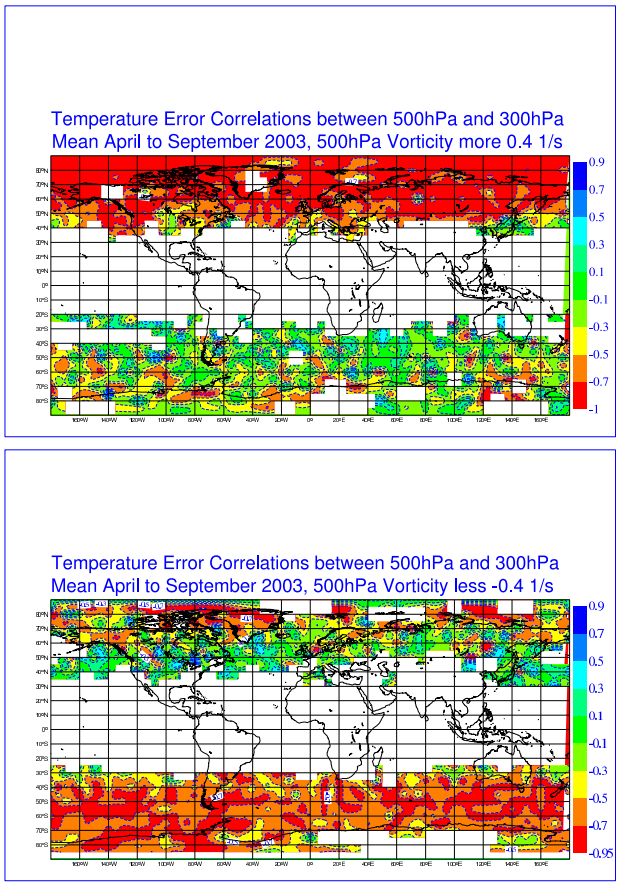

Figure 12. *As Fig. 11 (right), but for correlations between 500 hPa and 300 hPa.*

References

Berre L, Pannekoucke O, Desroziers G, Stefanescu SE, Chapnik B, Raynaud L. 2007. *A variational assimilation ensemble and the spatial filtering of its error covariances: increase of sample size by local spatial averaging*, Proceedings of the ECMWF workshop on flow–dependent aspects of data assimilation, 11–13 June 2007, pp. 151-168.

Bouttier JF. 1994. *Sur la prévision de la qualité des prévision météorologiques*, Thèse de doctorat de l'Université Paul Sabatier à Toulouse.

Buehner M. 2005. *Ensemble–derived stationary and flow–dependent background–error covariances: Evolution in a quasi–operational NWP setting*, Q. J. R. Meteorol. Soc. **131**, pp. 1013-1043.

Cohn CE. 1997. *An introduction to estimation theory*, J. Meteorol. Soc. Jap. **1B**, pp. 257-288

Courtier P. 1997. *Dual formulation of four–dimensional variational assimilation*, Quart. J. Roy. Met. Soc. **123**, pp. 2449-2461.

Dailey R, Barker E. 2001. *NAVDAS: Formulation and Diagnostics*, Mon. Wea. Rev. **192**, pp. 869-883.

Desroziers G, Ivanov S. 2001. *Diagnosis and adaptive tuning of observation–error parameters in a variational assimilation*, Quart. J. Roy. Met. Soc. **127**, pp. 1433-1452.

Evensen G. 1994. *Sequential data assimilation with a nonlinear quasi–geostrophic model using Monte Carlo methods to forecast error statistics*, J. Geophys. Res. **99 (C5)**, pp. 10 143-10 162.

Evensen G. 2003. *The Ensemble Kalman Filter: theoretical formulation and practical implementation*, Ocean Dynamics **53**, pp. 343-367.

Fisher M, Andersson E. 2001. *Developments in 4D–Var and Kalman filtering*, ECMWF Technical Memorandum **347**.

Hollingsworth A, Lonnberg P. 1986. *The statistical structure of short–range forecast errors as determined from radiosonde data. Part 1: The wind fields*, Tellus A **38**, pp. 111-136.

Houtekamer PL, Lefaivre L, Derome J, Ritchie H, Mitchell HL. 1996. *A system simulation approach to ensemble prediction*, Mon. Wea. Rev. **124**, pp. 1225-1242.

Lonnberg P, Hollingsworth A. 1986. *The statistical structure of short–range forecast errors as determined from radiosonde data. Part 2: The covariance of height and wind errors*, Tellus A **38**, pp. 137-161.

Kalman RE. 1960. *A new approach to linear filtering and prediction problems*, J. Basic Eng. **82**, pp. 35-45.

McNally AP. 2000. *Estimates of short–range forecast–temperature error correlations and the implication for radiance–data assimilation*, Q. J. R. Meteorol. Soc. **126**, pp. 361-373.

McNally AP. 2002. *A note on the occurrence of cloud in meteorologicaly sensitive areas and the implications for advanced infrared sounders*, Q. J. R. Meteorol. Soc. **128**, pp. 2251-2556.

Ott E, Hunt BR, Szunyogh I, Zimin AV, Kostelich EH, Corazza M, Kalnay E, Patil DJ, Yorke JA. 2004. *A Local Ensemble Kalman Filter for Atmospheric Data Assimilation*, Tellus A **56**, pp. 415-428.

Parrish DF, Derber JC. 1981. *The National Meteorological Center's Spectral Statistical Interpolation Analysis System*, Mon. Wea. Rev. **120**, pp. 1747-1763.

Raynaud L, Berre L, Desroziers G. 2008. *Spatial averaging of ensemble–based background–error variances*, Q. J. R. Meteorol. Soc. **134**, pp. 1003-1014.

Riishøjgaard, LP. 1998. *A direct way of specifying flow–dependent background error correlations for meteorological analysis systems*, Tellus A **50(1)**, pp. 42-57.

Watts PD, McNally AP. 1988. *The sensitivity of a minimum variance retrieval scheme to the values of its principle parameters*, Pp. 399-412 in Tech. Proc. 4th Int. TOVS Study Conf., 16–22 March 1988, Igls, Austria. CIMMS, University of Wisconsin–Madison, USA.

DOI: 10.1002/qj